JOURNAL OF MATERIALS SCIENCE 10 (1975) 52–62

Evolution of well-defined surface contour submitted to ion bombardment: computer simulation and experimental investigation

J. P. DUCOMMUN, M. CANTAGREL, M. MOULIN
Thomson-CSF, Laboratoire Central de Recherches, 91401 Orsay, BP No 10, France

The previously published theory of our model on the evolution of a surface contour under ion etching is recalled. Further improvements dealing with angular points of the profile shows that: angular points having straight trajectory may exist; and they can be found either by computation or by graphic method.

The experimental verification of the model is made on steps etched in silicon. SEM observations of the evolution of such steps under argon ion bombardment show good agreement between computed and experimental results.

1. Introduction

A theoretical model for the prediction of the evolution of a general surface ion beam sputtered has been expounded in an earlier communication [1] and compared to models proposed by Carter *et al.* [2-5] and Barber *et al.* [6]. In the present work, the theory is improved taking into account the equivalence of this model and the Frank's kinematic theory of dissolution of crystals applied to ion erosion by Barber.

Teodorescu and Vasiliu [7] have attempted an experimental investigation of the evolution of a copper surface during ion etching; however, the motion of the thermally etched defects on this surface was too complex to allow accurate conclusions. Smith *et al.* [8] has described the groove generation of ion etched $LiNbO_3$ through photoresist masks. Such observations are consistent with the model given in this paper, assuming that the shape of the sputtering yield of photoresists versus the incident angle is similar to the curve in Fig. 1. More precise measurements are necessary to confirm the model. They are detailed in the second part of this paper where well-defined steps engraved in silicon are ion etched and observed at grazing incidence with a scanning electron microscope.

2. Theoretical model

We assume that the evolution of a general surface contour by ion erosion (ion species and energy being fixed) is only dependent on (1) the geometrical form of the bombarded profile; (2) the sputtered material.

2.1. The hypothesis

(a) The surface contour is represented in a vertical (x 0 y) plane by the equation $y = f(x)$;y and its first derivative must be continuous.

(b) Planes (assumed to be straight lines in the (x 0 y) plane) move parallel to themselves by erosion.

(c) Secondary effects such as redeposition of sputtered materials and flux enhancement by ion reflection, etc, will not be considered.

(d) The bombarded material is homogeneous and isotropic. Therefore, the variation of sputtering yield S with angle of incidence θ can be depicted for a given material by a characteristic curve typified by the one in Fig. 1.

2.2. The principle (Fig. 2)

The initial contour (C) is considered as the envelope of a family (D) of straight lines. Ion beam erosion transforms this family (D) into a predictable new family (D'). The new surface contour (C') is the envelope of the transformed family (D').

2.3. Results and consequences

This principle leads to instantaneous transformation where at any time the slope of the tangent at any transformed point is equal to the

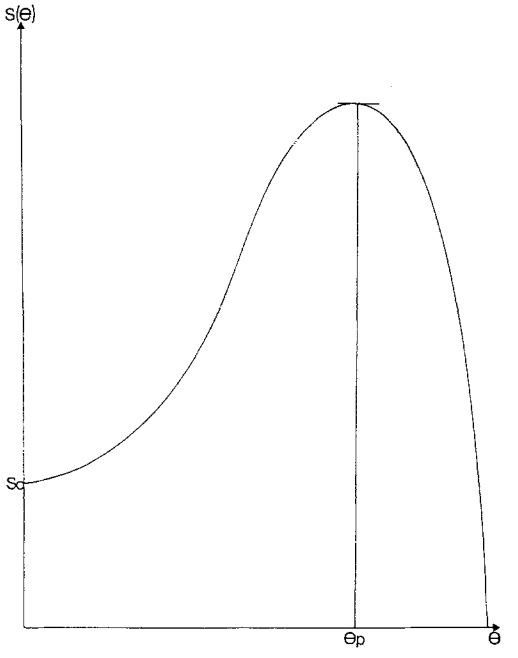

Figure 1 Typical variation of sputtering yield with angle of incidence.

initial slope of the tangent at the corresponding point.

Equations 1 and 2 give the transformed curve (C') of the initial curve (C).

$$x = x_i + \frac{\phi}{n} t \cos^2\theta \frac{dS(\theta)}{d\theta} \quad (1)$$

$$y = f(x_i) + \frac{\phi}{n} t \left[\sin\theta \cos\theta \frac{dS(\theta)}{d\theta} - S(\theta)\right] \quad (2)$$

where x_i, $f(x_i)$ is an arbitrary point of (C), x,y is the transformed point of (C'), ϕ is the ion flux in the negative $0y$ direction, n is the atomic density of the target, t is the time, S is the sputtering yield, θ is the angle of incidence.

Let us define

$$\Delta x = x - x_i = \frac{\phi}{n} t \cos^2\theta \frac{dS(\theta)}{d\theta}$$

$$\Delta y = y - f(x_i) = \frac{\phi}{n} t \left[\sin\theta \cos\theta \frac{d(S\theta)}{d\theta} - S(\theta)\right].$$

As θ is constant during the whole erosion time for each initial point $[x_i, f(x_i)]$, the trajectory of every initial point is a straight line. The slope of the trajectory is given by:

$$\frac{\Delta x}{\Delta y} = \frac{\cos^2\theta \, dS(\theta)/d\theta}{\sin\theta \cos\theta \, dS/d\theta - S(\theta)} = \tan\psi \cdot \quad (3)$$

As already shown [1] the present theory is equivalent to the model proposed by Barber *et al.* [6]. They have used the two kinematic theorems of crystal dissolution proposed by Frank [9] to predict the evolution of typical surface features submitted to ion bombardment.

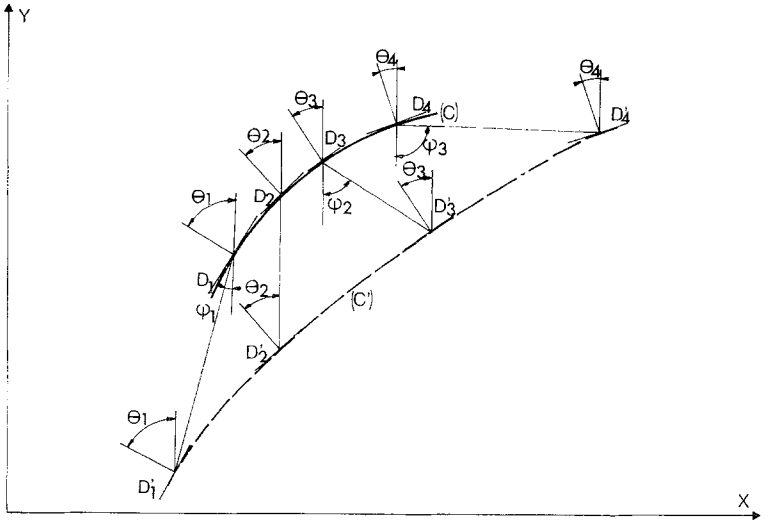

Figure 2 The principle of the evolution of a surface contour under ion bombardment.

The technique developed by Barber *et al.* from Frank's treatment uses the erosion slowness curve $1/V(\theta)$ plotted in polar form. This model allowed us to make additional interpretations of our results as given below.

(1) Cusps and double points exist on the transformed curve (C'). As already shown [1] the existence of such points is strictly dependent on two particular values of θ which are called θs_1 and θs_2. θs_1 and θs_2 are the inflection points on the erosion slowness curve $1/V(\theta)$.

(2) Starting from Equations 1 and 2 a computer program was proposed to draw (C') from (C) using a non-iterative method. The variation of S with θ must be introduced in this program in an analytical form.

The program was applied to the erosion of a sinusoidal profile and the following results were obtained.

(a) Such a profile, in relief above the horizontal plane, is progressively removed by erosion. For infinite time, the last stage of the evolution is the horizontal plane normal to the ion beam, this situation being a steady state.

(b) Such a surface without angular points is transformed by erosion into a contour with a predictable number of angular points.

(c) The number of angular points is strictly dependent on the eroded material through $S(\theta)$ and on the geometry of the initial profile through θ_M (maximum slope), θ_m (minimum slope) and R (radius of curvature).

(d) The type of evolution depends on the relative position of θ_M, θ_m, θs_1 and θs_2.

3. Study of angular points

3.1. Angular points on the initial profile

Following the hypothesis of our model, the function $y = f(x)$ which represents the initial profile (C) and its first derivative must be continuous. As the curves (C') are deduced from (C) by an instantaneous transformation, it is also possible to describe the initial profile by the following method.

(a) The initial curve is defined by a list of straight lines which are the tangents of a hypothetical curve described by a continuous function. The transformation therefore becomes identical to those previously described and the transformed curve (C') is always represented by the parametric Equations 1 and 2.

(b) If any angular point exists on the initial profile, planes of intermediate orientations are potentially present at this point according to the hypothesis of Frank [9]. At the angular point a list of straight lines with all intermediate slopes can be defined and the transformation previously used can be applied.

The results obtained with such profiles are identical to those obtained from a continuous profile [10].

3.2. Characterization of created angular points

According to Frank's theory the trajectory of the intersection between any two curves is not necessarily a straight line. In order to determine the conditions where the trajectory may be straight, let us consider the situation depicted in Fig. 3. The trajectory is a straight line if:

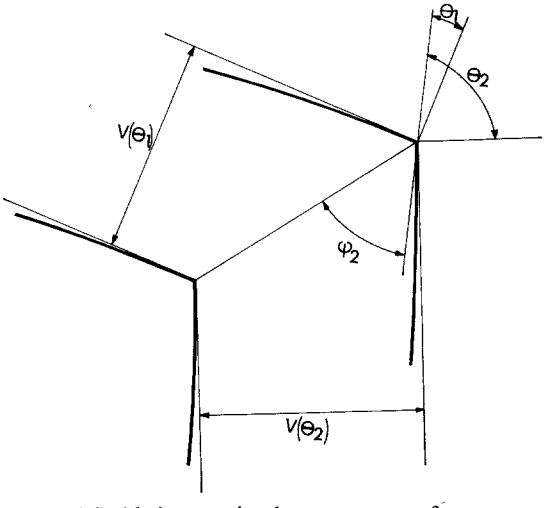

Figure 3 Stable intersection between two surfaces.

(a) the trajectory of the point A associated to the curve C_1 (with slope $\tan\theta_1$ at A) and the trajectory of the point A associated to C_2 (with slope $\tan\theta_2$ at A) must be superposed. This condition can be written:

$$\psi_1 = \psi_2 . \tag{4}$$

(b) The etching rates along the trajectory must be equal. Then

$$[V(\theta)/\cos(\theta + \psi)]_1 = [V(\theta)/\cos(\theta + \psi)]_2 \tag{5}$$

The resolution of Equations 4 and 5 gives values of θ_1 and θ_2 for which the trajectory is a straight line. In this condition we shall say that the angular point is stable.

In the same way we have determined the slope θ_i of any curves which give stable intersection angles with a plane of given orientation θ. This situation is depicted in Fig. 4.

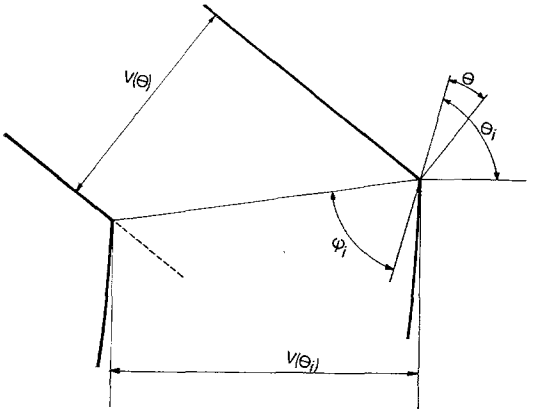

Figure 4 Stable intersection between a plane and a surface.

From the geometry of the system we obtain:

$$\frac{V(\theta)\cos[\psi(\theta_i) + \theta_i]}{V(\theta_i)\cos[\psi(\theta_i) + \theta]} = 1 . \qquad (6)$$

We can deduce θ_i for each θ from Equation 6, but a geometrical method can also be used. Consider Fig. 5. On the erosion slowness curve $1/V(\theta)$ used by Barber *et al.* consider the point A corresponding to the angle θ. From A we draw the tangents at the curve: points B and C are obtained. It can be easily shown that the values θ_i associated with these points are the solutions of Equation 6.

We now propose to verify the model on simple reproducible step profiles.

4. Experimental

All experiments were carried out with an apparatus previously described [11]. The ion energy is adjusted to 1 keV and the resulting ion current density is 0.6 mA cm^{-2}.

4.1. Choice of silicon as the bombarded material

Single crystal materials have a sputtering yield which generally depends on the crystallographic orientation of the bombarded surface. Anderson [12] has shown that semiconductor single crystals exhibit such variation when the temperature is higher than the critical temperature T_A. Conversely, when the target temperature is lower than T_A, ion bombardment gives rise to a stable amorphous layer.

Our silicon specimen shows an amorphous layer at the surface after bombardment at room temperature under observation by electron diffraction and RX topography. Measurements of sputtering yields for (100), (110) and (111) irradiated faces at different incidence angles give the same results. Silicon single crystal may, therefore, be considered in our experimental conditions to be homogeneous, isotropic material.

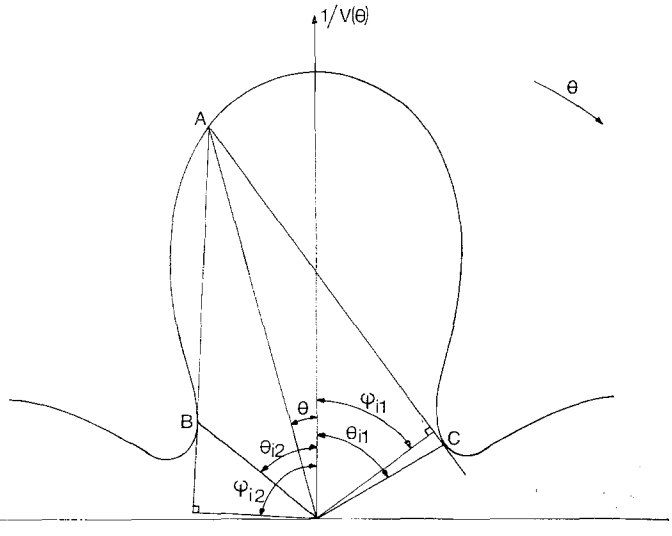

Figure 5 Graphical method to determine the angles of stable intersections.

The model can then be applied to ion bombardment of silicon.

4.2. Variation of etching rate and sputtering yield with angle of incidence

The etching rate and sputtering yield are calculated from the depth of steps ion-etched through photoresist masks. Depths are measured using a stylus instrument (Talystep).

$S(\theta)$ can be deduced from $V(\theta)$ through the relation

$$S(\theta) = \frac{n}{\phi}\frac{V(\theta)}{\cos\theta}.$$

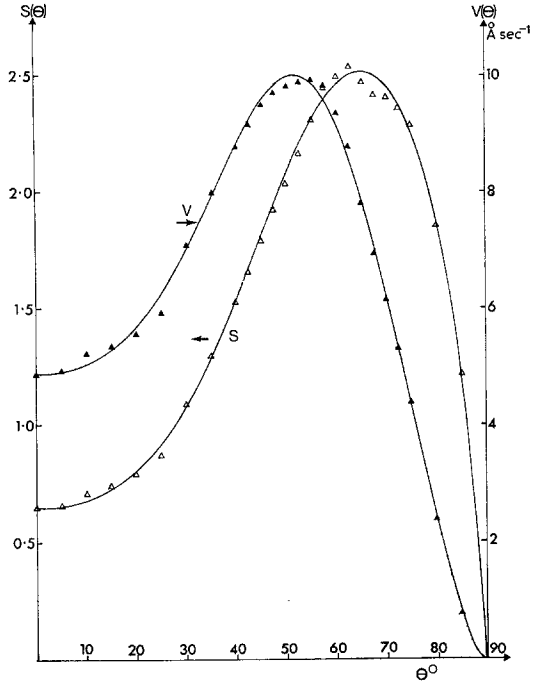

Figure 6 Variation of sputtering yield versus angle of incidence for silicon.

The measured values leads to the curves of figure 6. The accuracy on the measurements is 10% and is limited by the accuracy on the depth of the step, on the ionic density and on the angle of incidence.

V(θ) reaches a maximum for $\theta \simeq 50°$. At this point $V_{max} = 2.3\ V_0$ where V_0 is the etching rate at normal incidence. $S(\theta)$ reaches a maximum for $\theta \simeq 65°$. At this point $S(\theta_p)/S(\theta = 0) \simeq 4$. Our results at normal incidence are in good agreement with those previously published [13, 14].

As suggested by Stewart and Thomson [15], the peak in the sputtering yield occurs when the angle of incidence reaches the critical reflection angle θ_p given by Lindhard's formula

$$\frac{\pi}{2} - \theta_p = \sqrt{\left(\frac{5\pi a_0^2 Z_1 Z_2 E_R n^{2/3}}{(Z_1^{2/3} + Z_2^{2/3})E_1}\right)}$$

where a_0 is the hydrogen Bohr radius = 0.53 Å, Z_1 = ion atomic number, Z_2 = atomic number of target species, E_R = Rydberg energy = 13.6 eV, and E_1 = ion energy. This leads to $S(\theta_p)$ = 66° 54′ which is close to our experimental value.

We have shown in the theoretical section that $S(\theta)$ must be introduced into the simulation program in an analytical form. The best fitting of our results is obtained by the function

$$\begin{aligned} S(\theta) = {} & 18.738\,45\cos\theta - 64.659\,96\cos^2\theta \\ & + 145.199\,02\cos^3\theta - 206.044\,93\cos^4\theta \\ & + 147.317\,78\cos^5\theta - 39.899\,93\cos^6\theta . \end{aligned}$$

The intrinsic angles associated to this function are

$$\theta_p = 65° 06' \quad \theta s_1 = 37° 54' \quad \theta s_2 = 75°$$

4.3. Erosion of simple profiles

Steps are etched into silicon substrates by a method similar to that described by Cantagrel and Marchal [11]. Vanadium masks deposited by triode sputtering (height = 4000 Å) on silicon substrates are etched in 1.5×10^{-5} Torr oxygen pressure. The resulting profiles are observed by scanning electron microscopy at grazing incidence and are shown in Figs. 10a and 12a. The step is mainly composed of secant planes and the intersection at the top is perfectly defined. A groove exists at the foot of the step which can be attributed to a local increase in ion flux due to the reflection of incident ions on the side of the step.

4.4. Simulation

The initial profile can be defined by a list of secant segments with a good agreement with experimental observation.

Depth measured between the both horizontal planes is equal to 8000 Å.

The depth of the groove is 2000 Å.

The slope of the step is equal to tan 80° and the slope of the side of the groove is equal to tan 30°.

$S(\theta)$ is into the analytical form given by Equation 7.

The evolution of the initial step profile is then

obtained as a function of erosion time (Figs. 7 and 8). We can observe that:

(1) The angular point 0 gives rise to two angular points A and B which are stable. The angles associated with these points deduced from Equation 6 are 50° 18′ and 72° 25′ respectively. Between these points a rounded surface appears which grows at the expense of both the horizontal plane and the side of the step. The side is completely removed at $t \approx 8$ min.

(2) The angular point P gives rise to one angular point C which is also stable. The value deduced from Equation 6 is 6° 12′. The trajectories of B and C cross when 7.5 min $< t <$ 10 min. At this point D the angles are 72° 25′ and 6° 12′. These values do not verify the system of Equations 4 and 5, therefore the trajectory of D is not a straight line.

(3) The angular point Q gives rise to the angular point E. As potentially present planes have a slope between 0 and tan 30°, the stable angular point (corresponding to 50° 18′) cannot be created. E is then unstable and its trajectory is not a straight line.

(4) For $t \geqslant 10$ min the slope of the step obtained is constant as shown in Fig. 9. The value of this slope will be given later.

(5) The depth of the step remains constant during erosion.

(6) The width L_m (which is defined in Fig. 8) decreases with time and become zero for $t \approx 70$ min.

4.5. Comparison of theoretical and experimental results

Fig. 9 defines: H depth of the step, L_s width of the groove, H_c height of the rounded corner, L_c width of the rounded corner, and the angles at each angular point.

Samples are submitted to erosion at time intervals of 2.5 min until 15 min, and thereafter at 30, 45 and 60 min. SEM observations of this sequence are shown in Figs. 10 to 12.

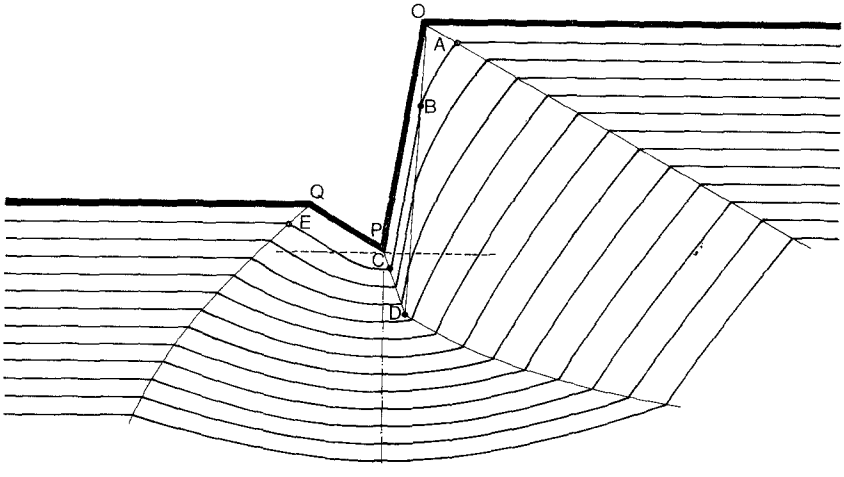

Figure 7 Evolution of a step during erosion: simulation.

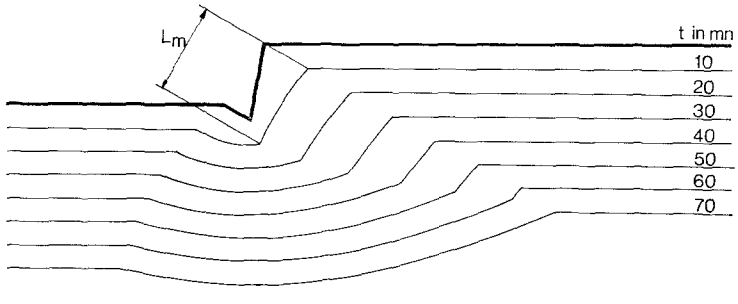

Figure 8 Further development of the surface shown in Fig. 7.

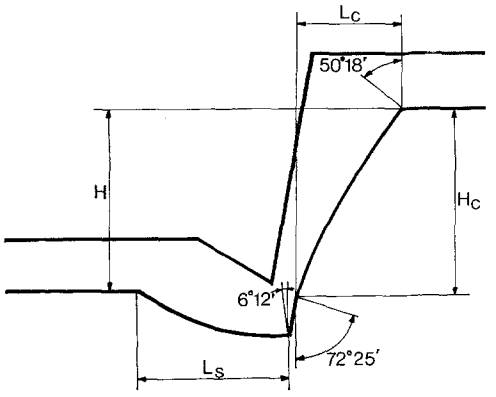

Figure 9 Characteristic angles and sizes of the eroded profile.

4.5.1. Number of angular points

The observation of angular points is difficult particularly in the groove. The four angular points cannot be seen simultaneously but, when $t \geqslant 10$ min, three angular points exist as shown in Fig. 12, as predicted.

4.5.2. Planes of particular orientations

Two angular points appear at the top of the step. Between these points a rounded surface grows which can be characterized by the values of H_c and L_c and the angles at angular points.

Table I shows that experimental and theoretical values are in good agreement.

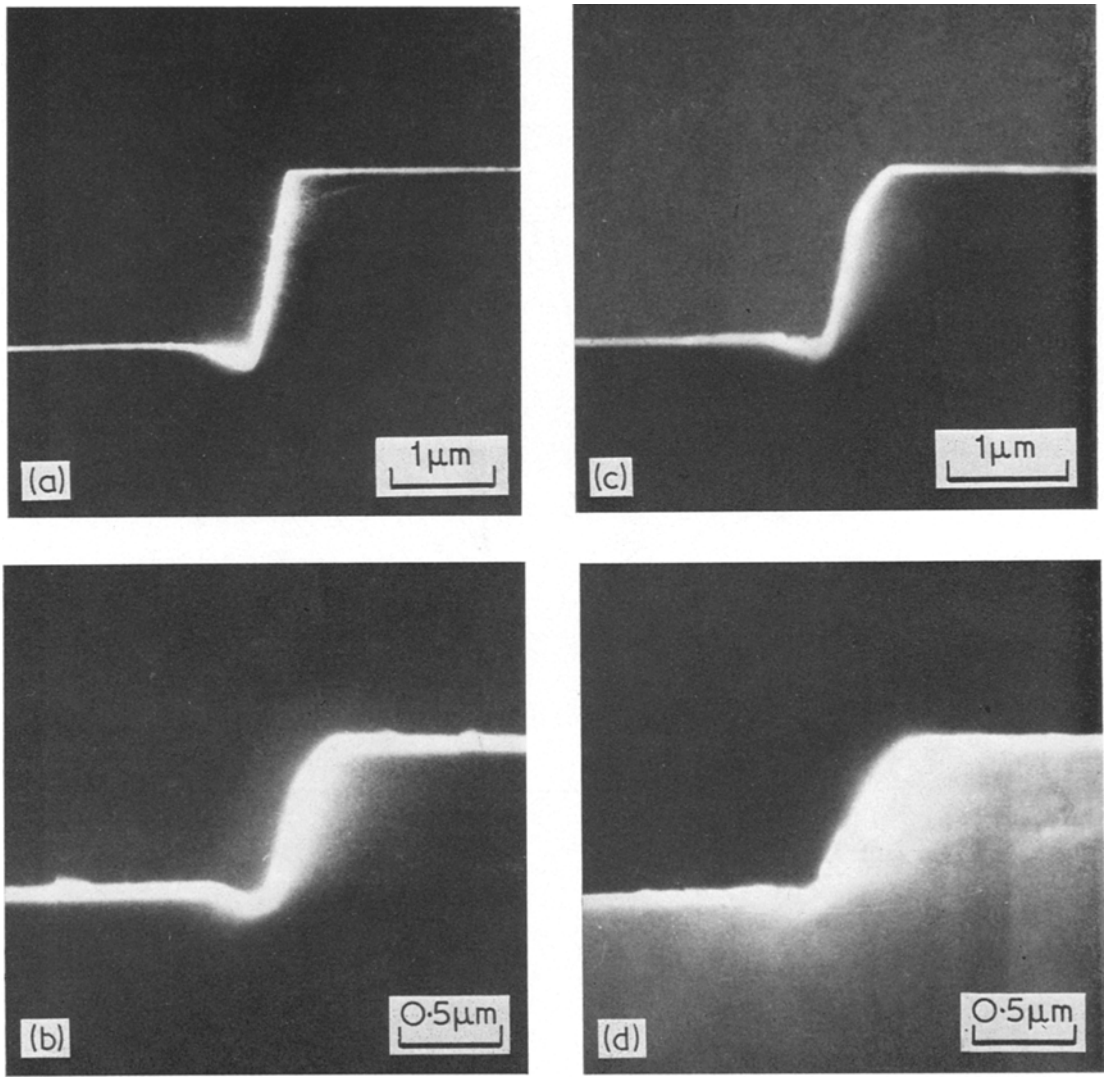

Figure 10 Experimental observations for time varying from 0 to 12.5 min with time intervals of 2.5 min.

4.5.3. Height of the step

Table IIa and b give the height H of the step which is found to be constant during erosion.

4.5.4. Development of the step for $t \geqslant 10$ min

Development of the step is characterized by the average slope (measured at half the height) and by the values of L_m. Table III gives these results versus erosion time. The measured value tends towards the theoretical values (tan 50° 18′) of the slope at the angular point A.

Conversely, the observed values of L_m are different from the theoretical predictions particularly for longer times. This may be due to

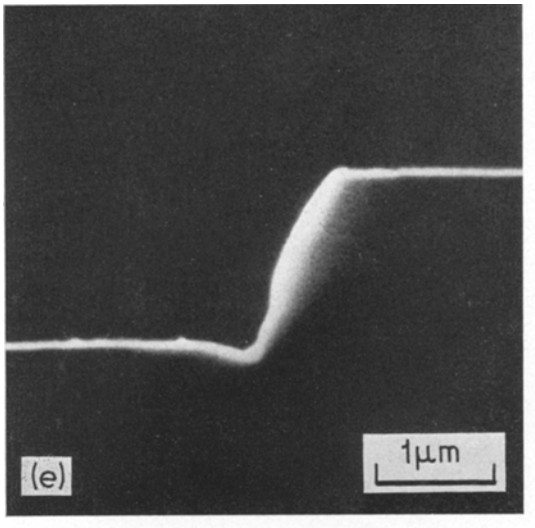

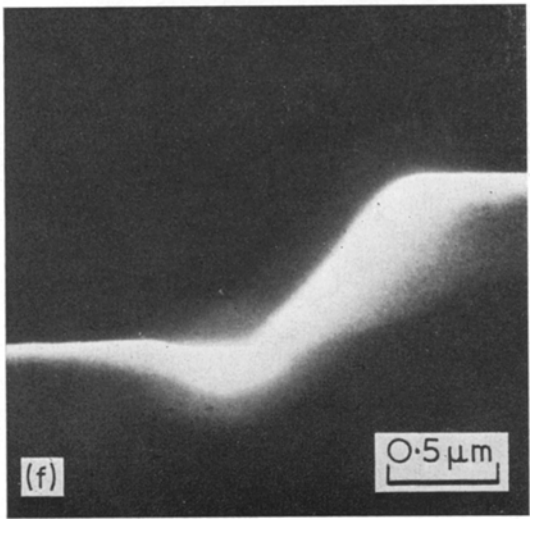

Figure 10 *continued*

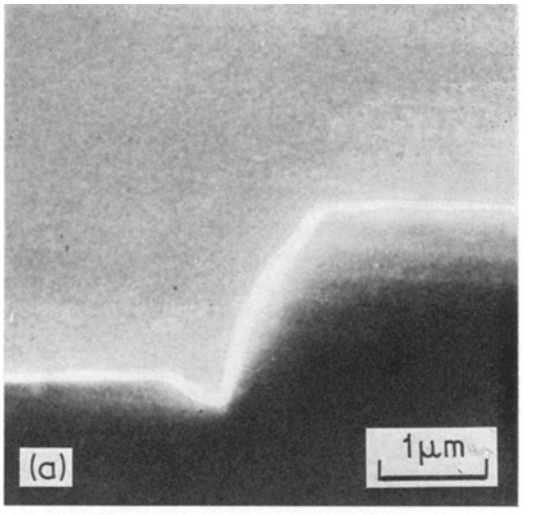

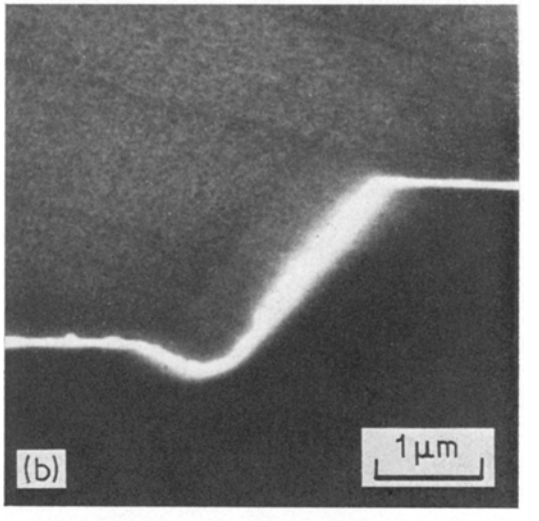

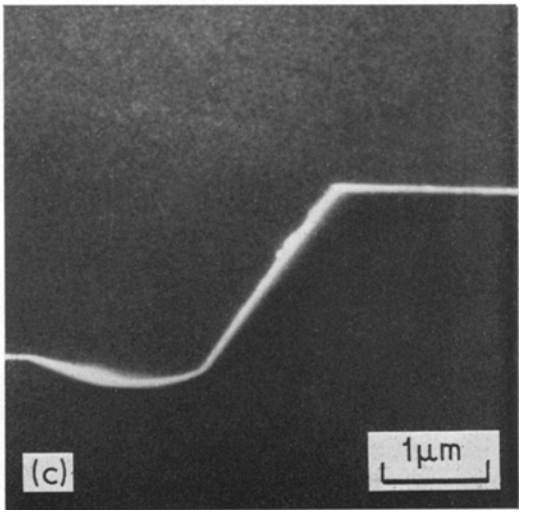

Figure 11 Experimental observations for t = 15, 30 and 45 min.

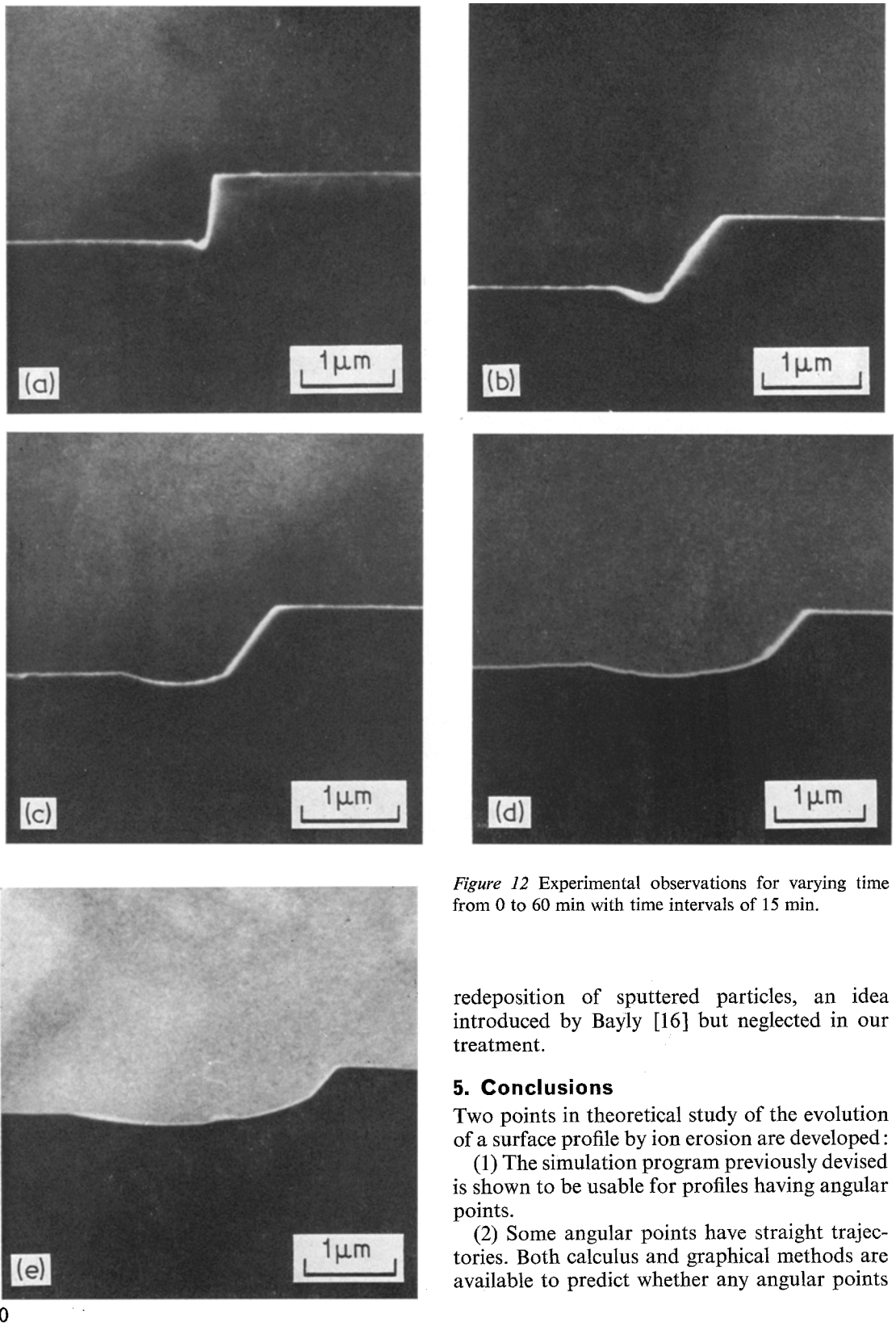

Figure 12 Experimental observations for varying time from 0 to 60 min with time intervals of 15 min.

redeposition of sputtered particles, an idea introduced by Bayly [16] but neglected in our treatment.

5. Conclusions

Two points in theoretical study of the evolution of a surface profile by ion erosion are developed:

(1) The simulation program previously devised is shown to be usable for profiles having angular points.

(2) Some angular points have straight trajectories. Both calculus and graphical methods are available to predict whether any angular points

TABLE I Measured values of characteristic sizes and angles

Time (min)	Figure	Method	H_c (Å)	L_c (Å)	Angles at high ang. point	Angles at low ang. point
2.5	11b	simul.	2700	1650	0–50° 18′	72° 25′–80°
		exp.	2700 ± 200	1600 ± 200	0–55° ± 5	70° ± 5°–80°
5	11c	simul.	5400	3300	0–50° 18′	72° 25′–80°
		exp.	4700 ± 300	2800 ± 300	0–50° ± 5	70° ± 5°–80°
10	11e	simul.	10800	6600	0–50° 18′	72° 25′–80°
		exp.	9500 ± 500	5600 ± 600	0–50° ± 5	75° ± 5°–80°

will have a straight trajectory and which particular slope will appear at these points.

An experimental verification of the proposed model is given. It is first shown that silicon satisfies the hypothesis of the model. Variation of the sputtering yield as a function of incident angle is then measured and fitted by an analytical function. Step profiles ion-etched into silicon single crystals are used as initial well-defined profiles. SEM micrographs of the surface evolution of steps under argon ion bombardment show that the convex angular point shifts into two angular points. A rounded surface is developed between these two points.

TABLE IIa Values of H during erosion.

	Time (min)					
	0	5	10	15	30	45
Figure	11a	11c	11e	12a	12b	12c
H (μm)	1.71	1.40	1.60	1.41	1.50	1.68

The measured size and angles of the rounded corner are in good agreement with the value given by computer simulation. The evolution of the bottom of the step differs slightly from that predicted due to secondary effects.

This model will be very useful when precise patterns are necessary. The starting mask may be designed taking into account the lateral shift which always occurs during ion etching and make possible the improvement of accuracy in engraving electronic or optical circuits.

References

1. J. P. DUCOMMUN, M. CANTAGREL and M. MARCHAL, *J. Mater. Sci.* **9** (1974) 725.
2. M. J. NOBES, J. S. COLLIGON and G. CARTER, *ibid* **4** (1969) 730.
3. G. CARTER, J. S. COLLIGON and M. J. NOBES, *ibid* **6** (1971) 115.
4. C. CATANA, J. S. COLLIGON and G. CARTER, *ibid* **7** (1972) 467.
5. G. CARTER, J. S. COLLIGON and M. J. NOBES, *ibid* **8** (1973) 1473.
6. D. J. BARBER, F. C. FRANK, M. MOSS, J. W. STEEDS, I. S. T. TSONG, *ibid* **8** (1973) 1030.

TABLE IIb Values of H during erosion

	Time (min)							
	0	2.5	7.5	12.5	15	30	46	60
Figure	13a	11b	11d	11f	13b	13c	13d	13e
H (μm)	0.76	0.68	0.71	0.72	0.78	0.68	0.63	0.66

TABLE III Slope and length of the side of the step versus time of erosion

Time (min)	Figure	Theoretical av. slope	Experimental av. slope	L_m theor. (μm)	L_m exp. (μm)
10	11e	58° 30′	60° ± 2°	1.16	1.13
15	13b	57°	55° ± 2°	1.13	1.05
30	13c	53°	54° ± 2°	0.93	0.88
45	13d	51° 30′	52° ± 2°	0.35	0.63
60	13e	50°	51° ± 2°	0.18	0.43

7. A. TEODORESCU and F. VASILU, *Rad. Effects* **15** (1972) 101.
8. H. I. SMITH, R. C. WILLIAMSON and W. T. BROGAN, I.E.E.E. Ultrasonics Symposium (1972) p. 198.
9. F. C. FRANK, "Growth and Perfection of Crystals" (Wiley, New York, 1958) p. 411.
10. J. P. DUCOMMUN, Thesis, Paris VI University (1974).
11. M. CANTAGREL and M. MARCHAL, *J. Mater. Sci.* **8** (1973) 1711.
12. G. S. ANDERSON, *J. Appl. Phys.* **37** (1966) 3455.
13. N. LAEGREID and G. K. WEHNER, *ibid* **32** (1961) 365.
14. L. I. MAISSEL and R. GLANG, "Handbook of thin film technology" (McGraw Hill, 1970) p. 4-40.
15. A. D. G. STEWART and M. W. THOMSON, *J. Mater. Sci.* **4** (1969) 56.
16. A. R. BAYLY, *ibid* **7** (1972) 404.

Received 24 June and accepted 8 July 1974.